

Nectin-2 Expression on Malignant Plasma Cells Is Associated with Better Response to TIGIT Blockade in Multiple Myeloma



Ester Lozano^{1,2}, Mari-Pau Mena¹, Tania Díaz¹, Beatriz Martín-Antonio^{1,3}, Sheila León¹, Luis-Gerardo Rodríguez-Lobato¹, Aina Oliver-Caldés¹, Maria Teresa Cibeira¹, Joan Bladé¹, Aleix Prat⁴, Laura Rosiñol¹, and Carlos Fernández de Larrea¹

ABSTRACT

Purpose: T-cell immunoreceptor with Ig and ITIM domain (TIGIT) blockade could represent an alternative therapeutic option to release the immune response in patients with multiple myeloma. Here we analyzed the expression of TIGIT and its ligands poliovirus receptor (PVR) and nectin-2 in the bone marrow (BM) of patients with monoclonal gammopathies and the efficacy of TIGIT blockade activating antimyeloma immunity.

Experimental Design: Expression levels of TIGIT and its ligands were characterized by flow cytometry and ELISA. TIGIT blockade was analyzed in *in vitro* functional assays with peripheral T cells. BM cells were studied with NanoString technology, real-time PCR, and *ex vivo* patient BM cell models.

Results: TIGIT and its ligands are highly expressed in the BM of patients with multiple myeloma, suggesting that may play a role in restraining immune activation. TIGIT blockade depleted FoxP3⁺

Tregs while increasing proliferation of IFN γ -producing CD4⁺ T cells from patients with multiple myeloma. PVR ligation inhibited CD8⁺ T-cell signaling and cell proliferation which could be overcome with anti-TIGIT mAb. However, BM cells showed a remarkable heterogeneity in immune signature. Accordingly, functional *ex vivo* BM assays revealed that only some patients respond to checkpoint blockade. Thus, response to TIGIT blockade correlated with low frequency of TIGIT⁺ cells and high nectin-2 expression on malignant plasma cells.

Conclusions: TIGIT blockade efficiently reinvigorated peripheral T cells from patients with multiple myeloma. However, in the BM, the efficacy of blocking anti-TIGIT mAb to achieve tumor cell death may depend on the expression of TIGIT and nectin-2, becoming potential predictive biomarkers for identifying patients who may benefit from TIGIT blockade.

Introduction

Multiple myeloma is a hematologic malignancy characterized by neoplastic proliferation of bone marrow plasma cells (BMPCs) that produce aberrant amounts of monoclonal Igs (1). Multiple myeloma is usually preceded by two asymptomatic conditions known as monoclonal gammopathy of undetermined significance (MGUS) and smoldering multiple myeloma (SMM), defined mainly when the percentage of BMPCs is higher than 10%, in both cases without end-organ damage (2, 3). The risk of progression from asymptomatic SMM to symptomatic disease is related to the proportion of BMPCs and the serum monoclonal protein level at diagnosis, among other prognostic factors (4, 5). Survival of patients with

symptomatic multiple myeloma has recently increased because of the discovery of therapeutic agents such as thalidomide, lenalidomide, bortezomib, and mAbs (anti-CD38, anti-CS1; refs. 6–8). However, most of the patients will eventually relapse after treatment (9), underlying the need for basic and translational research to achieve better therapeutic options.

Inhibitory immune checkpoints play an important role in tightly regulating the immune response against tumor cells (10, 11). Thus, blockade of coinhibitory receptors on immune cells or their ligands highly expressed on tumor cells has recently become innovative cancer immunotherapies. Antibodies targeting the negative immune checkpoints CTLA-4 and PD-1 have been approved to treat solid tumors and some hematologic malignancies (12–14). In patients with multiple myeloma, levels of inhibitory receptors CTLA-4, PD-1, LAG-3, and TIM-3 may indicate underlying mechanisms of T-cell dysfunction such as T-cell exhaustion (15) and immunosenescence that could be potentially reversible (16). Although initial data supported the rationale for PD-1 blockade to stimulate anti-multiple myeloma immunity, therapeutic antibody nivolumab as a single agent did not show a significant improvement in the treatment of patients with multiple myeloma (17–19) highlighting the need to investigate other immune regulatory pathways relevant in multiple myeloma.

Here, we analyzed the role of T-cell immunoreceptor with Ig and ITIM domain (TIGIT) and its ligands in regulating immune functions of T and NK cells from patients at sequential stages of multiple myeloma. TIGIT (previously known as VSIG9, VSTM3, and WUCAM) is an ITIM-bearing immunoreceptor expressed on NK cells and T cells upon activation. TIGIT interacts with the poliovirus receptor (PVR) and nectin-2 inhibiting NK-cell cytotoxicity (20) and promoting the generation of mature immunoregulatory dendritic

¹Department of Hematology, Hospital Clínic de Barcelona, Institut d'Investigacions Biomèdiques August Pi i Sunyer (IDIBAPS), Barcelona, Spain. ²Department of Cell Biology, Physiology and Immunology, Faculty of Biology, University of Barcelona, and Institute of Biomedicine of the University of Barcelona (IBUB), Barcelona, Spain. ³Josep Carreras Leukaemia Research Institute, Barcelona, Spain. ⁴Department of Medical Oncology, Hospital Clínic de Barcelona, Institut d'Investigacions Biomèdiques August Pi i Sunyer (IDIBAPS), Barcelona, Spain.

Note: Supplementary data for this article are available at Clinical Cancer Research Online (<http://clincancerres.aacrjournals.org/>).

Corresponding Authors: Ester Lozano, University of Barcelona and Institute of Biomedicine of the University of Barcelona (IBUB), Diagonal Av. 643, 3rd floor, Barcelona 08028, Spain. Phone: 346-2737-2188; E-mail: elozano@ub.edu; and Carlos Fernández de Larrea, Hospital Clínic de Barcelona, Villarroel Street, 170, Barcelona 08036, Spain. Phone: 349-3227-5428; E-mail: cfernan1@clinic.cat

Clin Cancer Res 2020;26:4688–98

doi: 10.1158/1078-0432.CCR-19-3673

©2020 American Association for Cancer Research.

Translational Relevance

TIGIT blockade is currently under investigation in ongoing clinical trials to treat several cancer types including multiple myeloma. In multiple myeloma, *in vitro* studies with CD8⁺ T cells as well as animal models have provided initial promising results. However, bone marrow (BM) microenvironment heterogeneity among patients may determine the response to immune checkpoint blockade. Here, we showed high expression of TIGIT and its ligands nectin-2 and poliovirus receptor (PVR) in the BM from patients with multiple myeloma. Our mechanistic studies proved that TIGIT blockade prevented PVR inhibitory signaling, achieving patient T-cell reinvigoration and Treg depletion. However, gene expression analysis revealed a remarkable heterogeneity in tumor microenvironment, consistent with different levels of response to TIGIT blockade found in *ex vivo* models. Better responses to TIGIT blockade correlated with higher expression of nectin-2 and lower frequency of TIGIT⁺ cells in BM. This study provides insights for TIGIT blockade in multiple myeloma in terms of molecular mechanisms and useful biomarkers to predict treatment response.

cells (21). We previously described that agonistic antibodies against TIGIT triggered an intrinsic inhibitory signal for T cells (22, 23). Indeed, TIGIT exerts multiple mechanisms of peripheral tolerance such as direct inhibition of T-cell proliferation, induction of IL10, and blockade of CD226-positive costimulatory signaling (23, 24). Conversely, the Th1-associated receptor CD226 also binds to PVR and nectin-2 delivering a stimulatory signal for T-cell proliferation and IFN γ production (25, 26). Importantly, regulatory FoxP3⁺ T cells (Tregs) highly express TIGIT which is associated to increased regulatory function and secretion of immunosuppressive cytokines (27).

TIGIT has become an attractive target for cancer immunotherapy (28, 29). Administration of blocking anti-TIGIT mAbs achieved tumor regression in several murine cancer models (30, 31), including the aggressive Vk12653 multiple myeloma model (32). In this study, we aim to investigate the relevance of TIGIT and its ligands in regulating antitumor immunity in patients at sequential stages of monoclonal gammopathies, from asymptomatic condition MGUS, SMM, symptomatic multiple myeloma and in patients who have achieved complete remission (CR) after treatment. A better understanding of TIGIT axis in human tissues at different stages of the disease will be necessary to identify patients who may potentially benefit from these new cancer immunotherapies.

Materials and Methods

Patient cohorts

BM aspiration samples were collected from 27 patients with MGUS, 15 with SMM, 24 patients with newly diagnosed multiple myeloma (NDMM), 25 refractory/relapsed patients with multiple myeloma (RRMM), and 22 patients with multiple myeloma in CR diagnosed at the Amyloidosis and Myeloma Unit in the Department of Hematology (Hospital Clínic of Barcelona). Clinical and lab characteristics of the recruited patients are summarized in Supplementary Table S1. In addition, for comparison purposes, we collected BM samples from nine individuals (average age = 67.9 years; male/female = 2/7) who were negative for any hematologic malignancy including monoclonal gammopathies whose BM aspirates were performed because of the

following symptoms: anemia ($n = 4$), mild leukopenia ($n = 3$), and mild neutropenia ($n = 2$). Sample collection and clinical record review were performed after informed written consent in accordance with the Declaration of Helsinki. Study protocol was approved by the Institutional Review Board at Hospital Clínic of Barcelona. Patients were diagnosed according to standard International Myeloma Working Group criteria (33).

Flow cytometry analysis

Immune cell subset characterization from patient BM samples was performed with eight-color panels of antibodies using a BD FACSCanto II flow cytometer and FACSDiva software (BD Biosciences). Complete list of antibodies and clones can be found in the Supplementary Materials and Methods section. At least 500,000 events per sample were acquired and data were analyzed with FlowJo Software v.10 (BD Biosciences).

ELISA

Concentrations of soluble TIGIT ligands PVR and nectin-2 (PVRL2) were measured in BM plasma using PVR ELISA Kit (ABIN417672, Cloud-Clone Corp.) and PVRL2 ELISA Kit (ABIN4883871, RayBiotech Inc.) from Antibodies-online. LEGEND MAX Human IFN γ ELISA Kit (BioLegend) was used to quantify IFN γ in culture supernatants.

Phenotypic and functional assessment of CD4⁺ T cells from patients with multiple myeloma

Peripheral blood mononuclear cell (PBMC) from patients were obtained by density gradient centrifugation (Ficoll, Sigma-Aldrich). Untouched CD4⁺ T cells were isolated with Human CD4⁺ T Cell Isolation Kit and the autoMACS Pro Separator from Miltenyi Biotec (Bergisch Gladbach). CD4⁺ T cells were preincubated in 96-well U-bottom plates for 30 minutes in the presence of immobilized anti-TIGIT (MBSA43) functional grade or IgG1k isotype control from Thermo Fisher Scientific. After preincubation, IL2 (10 U/mL) and MACSiBead particles with CD2, CD3, and CD28 antibodies (Treg Suppression Inspector, Miltenyi Biotec) were added to wells. At day 2, cells were collected and stored with TRIzol reagent at -80°C for gene expression analysis. At day 3, cells were stimulated with phorbol myristate acetate (50 ng/mL), ionomycin (250 ng/mL), and brefeldin A (BioLegend) for 4 hours and stained with LIVE/DEAD Fixable Violet Dead Cell Stain Kit (Thermo Fisher Scientific). Cells were fixed with FoxP3 Transcription Factor Staining Buffer Kit (Thermo Fisher Scientific) and intracellular cytokine staining was measured with AlexaFluor 488 anti-human IFN γ (clone B27) from Biolegend. Proliferating cells were stained with AlexaFluor 700 anti-Ki67 (B56) from BD Biosciences.

Detection of phosphorylation state of cell signaling pathways by antibody arrays

EasySep Human CD8⁺ T Cell Isolation Kit (STEMCELL Technologies Inc.) was used for negative selection of CD8⁺ T cells from PBMC. Changes in phosphorylation of intracellular mediators of T-cell signaling pathways were assessed in CD8⁺ T cells from healthy donors, incubated onto immobilized PVR (200 ng/mL) for 18 hours and then stimulated with CD2/CD3/CD28 MACSiBead particles for 30 minutes. Cell lysates were incubated on Human MAPK Phosphorylation Arrays C1 (AAH-MAPK-1-2, RayBiotech, Inc.) overnight at 4°C according to manufacturer's instructions and phosphorylated proteins were detected by chemiluminescence on a ImageQuant LAS 4000 imaging system (GE Healthcare).

Proliferation assays

Isolated CD8⁺ T cells from healthy donors and patients with multiple myeloma were labeled with carboxyfluorescein succinimidyl ester (CFSE) and incubated onto immobilized PVR in the presence of blocking anti-TIGIT (10 µg/mL) or isotype control. After 4 days, percentage of CFSE^{low} CD8⁺ T lymphocytes was analyzed by flow cytometry.

Gene expression analysis

Total RNA was isolated from TRIzol reagent and retrotranscribed using High Capacity cDNA Reverse Transcription Kit (Thermo Fisher Scientific). Reactions with Taqman Universal PCR Master Mix and specific probes were run on a 7900 Real-Time PCR System (Thermo Fisher Scientific). Values are represented as the difference in C_t values normalized to endogenous control β-glucuronidase (*GUSb*) for each sample as per the following formula: Relative RNA expression = 1,000 × 2^{-ΔC_t} as described previously (11).

NanoString immune gene expression panel analysis

RNA expression was measured with the nCounter technology, preparation and analyses were performed according to the manufacturer's protocol (NanoString Technologies, Inc.). Two hundred nanograms of RNA per sample was loaded and run on the HuV1_Cancer Immu_v1_1_Nanostring for analysis of the NanoString PanCancer Immune Profiling Panel of 770 genes. Raw gene counts were log₂ transformed and normalized to the geometric mean of 30 housekeeping genes included in the panel with the nSolver v4 software.

Ex vivo BM functional assays

BM mononuclear cells were isolated by Ficoll density gradient centrifugation and cultured in the presence of 10 µg/mL of human anti-TIGIT mAb (MBSA43) or IgG1k isotype control, both from Thermo Fisher Scientific. After 18 hours, absolute quantification of PCs (CD45⁺CD38⁺CD138⁺) was performed by flow cytometry with addition of 50 µL of CountBright Absolute Counting Beads (Thermo Fisher Scientific) per well. Cells were acquired on a BD FACSCanto II cytometer and data were analyzed with FlowJo Software v.10 (BD Biosciences).

Statistical analysis

Brown–Forsythe ANOVA tests followed by Games–Howell multiple comparison tests were used when SDs were significantly different in independent groups of patients. Pearson correlation coefficients (*r*) were used to assess correlations as indicated in the text. Wilcoxon signed-rank test was used to analyze changes in IFNγ production after treatment with anti-TIGIT mAb. Differences were considered statistically significant at *P* values less than 0.05. All statistical analyses were performed using GraphPad Prism, v8.0.1 (GraphPad Software, Inc.).

Results

Negative immune checkpoint TIGIT is highly expressed on BM immune cells at sequential stages of monoclonal gammopathies

To investigate whether TIGIT could represent a useful target to activate the anti–myeloma immune response against malignant PCs, we first quantified the frequency of immune cells expressing TIGIT in BM from patients at sequential stages of multiple myeloma as well as patients without any neoplastic malignancy (Ctrl). As shown in Fig. 1, cytotoxic CD8⁺ T cells and NK cells expressed significantly higher levels of TIGIT compared with CD4⁺ T cells in all studied groups.

Interestingly, patients with the premalignant condition SMM, showed significantly lower TIGIT levels on CD4⁺ T cells (Fig. 1C) which suggest a role for TIGIT⁺ CD4⁺ T cells in pathophysiology of SMM. In line with these results, we also found that the number of malignant PCs in patients with multiple myeloma positively correlated with TIGIT expression in both CD4⁺ T cell and NK subsets (Fig. 1D). Interestingly, the frequency of TIGIT⁺CD4⁺ T cells in the BM in patients with NDMM is significantly higher compared with patients with refractory multiple myeloma (Supplementary Fig. S1). Taken together, our data support the concept that TIGIT may play a role in the BM of patients with multiple myeloma.

TIGIT ligands PVR (CD155) and nectin-2 (CD112) are highly expressed in BM cells in multiple myeloma

To assess whether TIGIT inhibitory signaling takes place in the BM, we next characterize expression patterns of the TIGIT ligands PVR (CD155) and nectin-2 (CD112) in BM cells from patients at sequential stages of disease. We found that the ITIM-bearing receptor PVR was highly expressed on several subsets of CD138⁺ BM cells including CD14⁺ monocytes (Fig. 2A and B). Malignant PCs can also express PVR in a lesser extent but no differences were found in patients with multiple myeloma compared with MGUS (Fig. 2B). On the contrary, most of BM cells expressed low levels of nectin-2, PCs in SMM showed higher expression than in NDMM but differences did not reach statistical significance. Moreover, expression of both receptors positively correlated in PCs from patients with multiple myeloma (Fig. 2C).

Because both ligands can be found in soluble form, we next quantified their concentration levels in BM plasma. Although both ligands were found in high concentrations, no significant differences were detected in multiple myeloma compared with MGUS (Fig. 2D and E). However, when we analyzed paired samples from patients with symptomatic multiple myeloma and in CR after treatment, we found a significant decrease of PVR levels in CR that was associated with a significant increase in soluble nectin-2 (Fig. 2D and E). Hence, our data show that TIGIT and their ligands are highly expressed in the BM suggesting that this negative signaling pathway may take place in the BM of patients with multiple myeloma. These results raised the question of whether TIGIT blockade could activate immune cells to target malignant PCs in patients with myeloma.

TIGIT blockade decreases frequency of Tregs and increases IFNγ production by CD4⁺ T cells from patients with multiple myeloma

Immune cells from patients with multiple myeloma may show defective effector functions leading to a heterogeneous range of immunosuppression degree at the time of diagnosis. Accordingly, we observed that TIGIT⁺ CD4⁺ T cells in BM expressed significantly lower levels of the activation marker CD38 compared with TIGIT[−] CD4⁺ T cells in individuals with MGUS, SMM, and NDMM (Fig. 3A). We next wanted to evaluate whether TIGIT blockade could reinvigorate T-cell effector functions in CD4⁺ T cells from patients with symptomatic multiple myeloma. Because of the limited volume of BM sample for diagnostic purpose, the effect of the neutralizing anti-TIGIT mAb was tested in CD4⁺ T cells isolated from peripheral blood from healthy donors and patients with MGUS, SMM, NDMM, and RRMM. Thus, CD4⁺ T cells incubated in the presence of blocking anti-TIGIT mAb for 48 hours showed significant downregulation of TIGIT mRNA and key genes for regulatory T-cell function such as Treg master transcription factor FoxP3 and immunosuppressive cytokine IL10 (Fig. 3B). Conversely, TIGIT blockade resulted in increased IFNγ

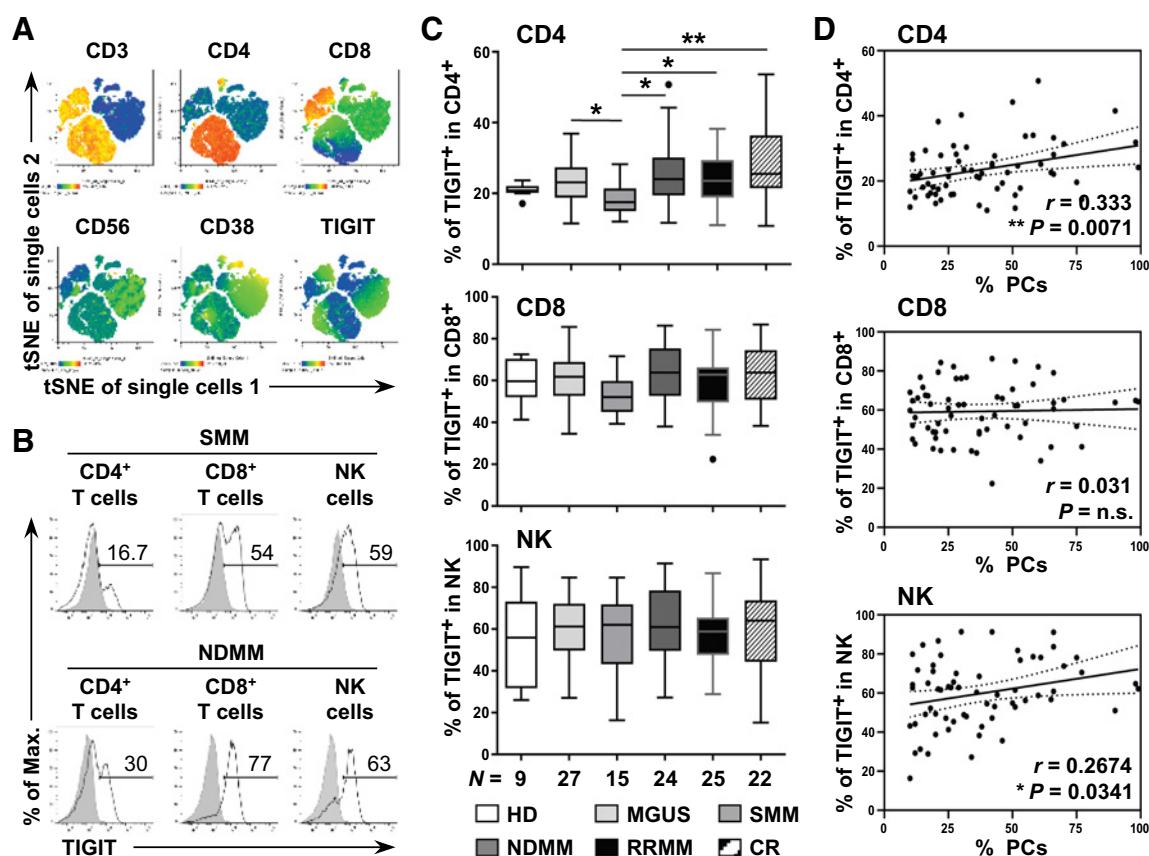


Figure 1.

Negative immune checkpoint TIGIT is highly expressed on BM immune cells at different stages of multiple myeloma progression. **A**, t-SNE plots showing indicated markers in BM cells from representative patient with multiple myeloma. **B**, Representative histograms of TIGIT expression analyzed by multicolor flow cytometry on BM CD4⁺ T cells (gating on CD45⁺CD3⁺CD8⁻CD4⁺), CD8⁺ T cells, and NK cells (gating on CD45⁺CD3⁻CD8⁻CD4⁻CD38^{med}CD56⁺). Complete gating strategy is not shown. TIGIT expression (solid line) versus isotype control (filled histogram) in two representative patients with SMM and NDMM. **C**, Summary data of coinhibitory receptor TIGIT expression on CD4⁺ T cells, CD8⁺ T cells, and NK cells in BM aspirates from asymptomatic patients with MGUS ($n = 27$), patients with SMM ($n = 15$), untreated patients with newly diagnosed multiple myeloma ($n = 24$), patients with refractory/relapsed multiple myeloma ($n = 25$) and patients with multiple myeloma in complete remission (CR) after treatment ($n = 22$); as well as individuals without any hematologic malignancy (Ctrl; $n = 9$). Box plots indicate mean and SEM values. P values were determined by Brown-Forsythe ANOVA test followed by Games-Howell multiple comparison tests (*, $P < 0.05$; **, $P < 0.01$). **D**, Pearson correlation coefficients (r) were used to assess correlations between TIGIT-expressing cells and frequency of malignant PCs in BM aspirates from 64 patients with multiple myeloma (SMM $n = 15$, NDMM $n = 24$, RRMM $n = 25$). Each data dot represents an individual patient (**, $P < 0.01$; $P = n.s.$, nonsignificant).

mRNA expression in patients with newly diagnosed multiple myeloma (Fig. 3B).

To investigate whether TIGIT blockade may affect the balance T effector/Treg cell, we next analyzed cell viability, intracellular expression of the proliferation-associated marker Ki67, and the transcription factor FoxP3 by flow cytometry. After the confirmation that the presence of anti-TIGIT mAb did not affect cell viability and gating on viable cells, we found a remarkable increase in Ki67⁺ cells in FoxP3⁻ cells while the percentage of FoxP3⁺ Tregs were significantly reduced in the presence of anti-TIGIT in healthy donors, patients with MGUS and NDMM (Fig. 3C). Furthermore, intracellular staining after phorbol myristate acetate/ionomycin restimulation demonstrated that neutralizing TIGIT signaling increased IFN γ expression without significant changes in TNF α production (Fig. 3C). Increased secretion of IFN γ after TIGIT blockade was also confirmed in the supernatants of these experiments by ELISA (Fig. 3D). To sum up, our results showed that TIGIT blockade reduced the number of FoxP3⁺ Tregs while

increasing T eff proliferation and IFN γ production by CD4⁺ T cells from patients with multiple myeloma.

TIGIT blockade potentiates proliferation of cytotoxic CD8⁺ T cells from patients with multiple myeloma

Unlike CD4⁺ T cells, TIGIT⁺ CD8⁺ T cells showed higher levels of CD38 expression than TIGIT⁻ CD8⁺ T cells in the BM of patients with MGUS, NDMM, and patients in CR (Fig. 4A). To better understand how TIGIT negative signaling regulates CD8⁺ T-cell function, we studied proliferation and phosphorylation state of intracellular mediators of healthy donor CD8⁺ T cells in the presence of TIGIT ligand PVR. As expected, PVR binding triggered a significant inhibition of T-cell proliferation while blocking anti-TIGIT mAb restored cell growth indicating that the inhibitory effect was due to specific interaction with TIGIT (Fig. 4B). No significant differences in proliferation were found in the absence of PVR. Furthermore, T cells cultured onto recombinant PVR showed a remarkable decrease in phosphorylation of intracellular mediators, including key components of the signaling

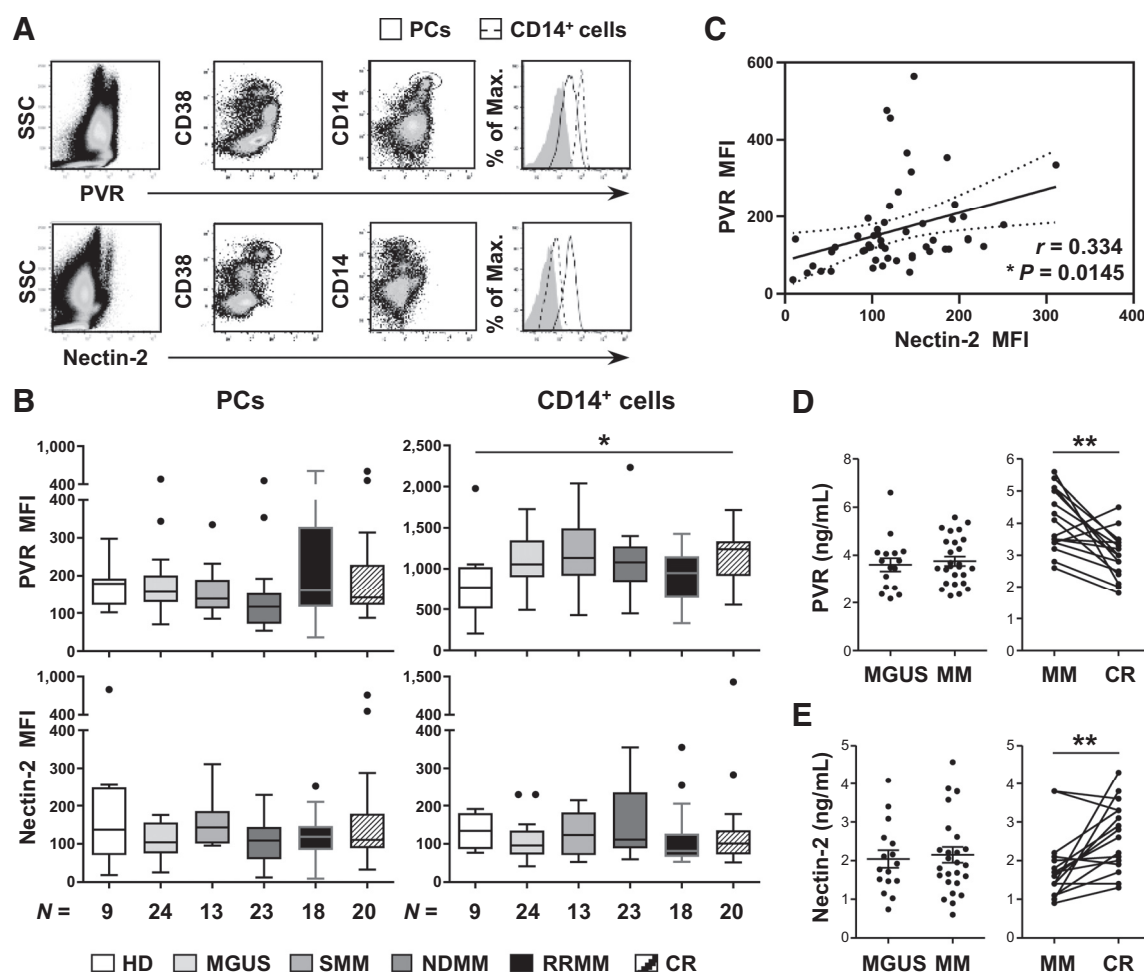


Figure 2.

TIGIT ligands PVR (CD155) and nectin-2 (CD112) are highly expressed in BM cells in multiple myeloma. **A**, Representative dot plots and histograms of PVR and nectin-2 expression on BM PCs (solid line) and CD14⁺ monocytes (dashed line) versus isotype control (filled histogram). **B**, Summarized mean fluorescence intensity (MFI) values of PVR and nectin-2 expression on PCs and CD14⁺ monocytes in patients with MGUS, patients with SMM, untreated patients with newly diagnosed multiple myeloma, patients with refractory/relapsed multiple myeloma, and patients with multiple myeloma in complete remission (CR) after treatment; as well as individuals without any hematologic malignancy (Ctrl; $n = 9$). Kruskal-Wallis test (*, $P < 0.05$). **C**, Positive correlation between PVR and nectin-2 expression on PCs from patients with multiple myeloma (SMM $n = 13$, NDMM $n = 23$, RRMM $n = 18$). **D**, Soluble PVR concentration measured by ELISA in BM plasma from patients with MGUS ($n = 20$) compared with 20 patients with multiple myeloma (NDMM $n = 16$, RRMM $n = 4$). Paired data comparing PVR levels in patients with NDMM and after achieving CR ($n = 14$). **E**, Soluble nectin-2 concentrations measured by ELISA in the same paired samples. Two-tailed paired t test (**, $P < 0.01$).

transduction pathways such as Akt (Fig. 4C). Similarly, PVR also triggered an inhibitory signal into the CD8⁺ T cells from patients with multiple myeloma that led to a significant decrease in T-cell proliferation. TIGIT blockade efficiently restored cell growth indicating that PVR inhibitory signal depends on TIGIT ligation (Fig. 4D and E). Therefore, our data indicate that both peripheral CD4⁺ and CD8⁺ T cells from patients with multiple myeloma can be stimulated by neutralizing intrinsic TIGIT signaling.

High levels of TIGIT gene expression are associated to upregulation of genes involved in T-cell function and cytotoxicity in the BM from patients with multiple myeloma

Given that our functional studies showed that TIGIT blockade can activate PB circulating T cells from patients with multiple myeloma, we next wanted to focus on immune cell composition and function in the tumor microenvironment. To this end, we first analyzed samples of

CD138-depleted BM cells from 12 patients with multiple myeloma by using NanoString technology, we quantified the abundance of mRNA with a panel of 770 immune-related genes including genes involved in the innate and adaptive immune response from 24 types of immune cells from the human repertoire. As shown in Fig. 5, we found upregulation of 262 genes out of 291 differently expressed genes in patients with multiple myeloma with high levels of TIGIT expression in BM compared with those with low TIGIT levels, indicating that the expression of this receptor could act as a marker of an immune signature in the BM of a subgroup of patients. (Fig. 5A and B; Supplementary Table S2). Hence, functional pathway analysis showed higher gene signature scores for genes encoding for interleukins (*IFNL1*, *IL32*, *TGFB1*, *IL15*, *IFNA7*), antigen processing (*HLA-B*, *HLA-A*, *PSMB7*), and cytotoxicity (*GZMM*, *CD8A*) in samples with higher TIGIT expression (Fig. 5C and D). Because TIGIT is highly expressed on FoxP3⁺ Tregs, we also found higher expression of

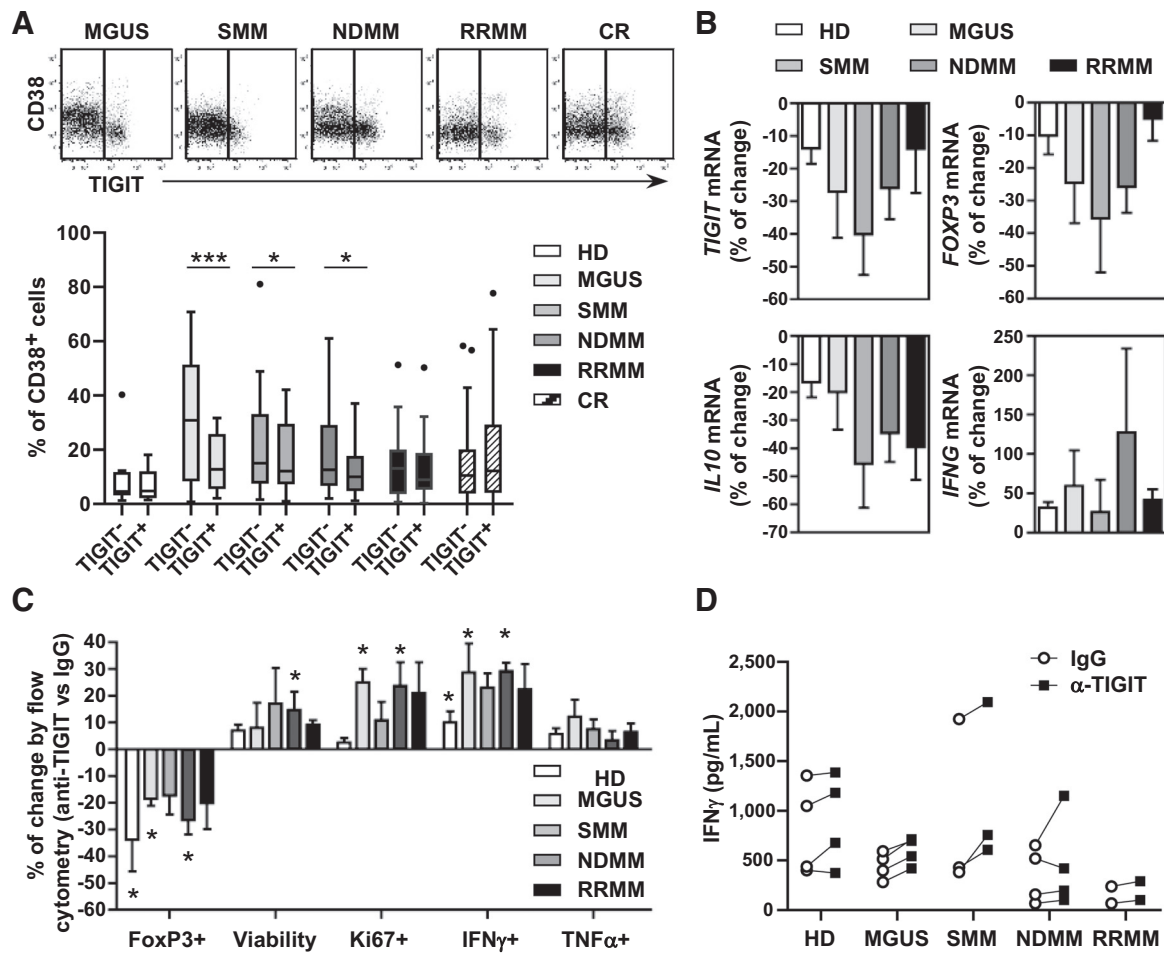


Figure 3.

TIGIT blockade promotes T-cell activation and increases IFN γ production by CD4⁺ T cells from patients with multiple myeloma. **A**, Surface expression of activation marker CD38 on BM TIGIT⁻ and TIGIT⁺ CD4⁺ T cells in patients with MGUS ($n = 27$), SMM ($n = 15$), newly diagnosed multiple myeloma ($n = 24$), relapsed/refractory multiple myeloma ($n = 25$), and patients with multiple myeloma in CR ($n = 22$). Wilcoxon matched-pairs signed-rank test (*, $P < 0.05$; ***, $P < 0.001$). **B**, CD4⁺ T cells were isolated from peripheral blood from healthy donors ($n = 4$), patients with MGUS ($n = 4$), SMM ($n = 3$), NDMM ($n = 4$), RRMM ($n = 2$), preincubated with RPMI medium with 10% human serum, in the presence of immobilized neutralizing anti-TIGIT mAb (10 $\mu\text{g}/\text{mL}$) or isotype control. After 1 hour, cells were stimulated with CD2/CD3/CD28 MACSBead particles (bead-to-cell ratio 1:1) and IL2 (10 U/mL). After 48 hours, changes in gene expression were quantified by real-time PCR. Values obtained after TIGIT blockade were normalized to isotype control (as 100%) and percentages of change are depicted. Bar graphs show mean \pm SEM. **C**, CD4⁺ T cells were cultured in the same conditions as in **B** and restimulated with phorbol myristate acetate/ionomycin in the presence of brefeldin A for 4 hours. Cells were first stained with LIVE/DEAD staining to quantified cell viability. Gating on viable cells, intracellular expression of IFN γ and TNF α were assessed. Summarized data of percentages of change in FoxP3, viability, Ki67, IFN γ , and TNF α after TIGIT blockade are depicted for healthy donors ($n = 4$), patients with MGUS ($n = 4$), SMM ($n = 3$), NDMM ($n = 4$), and RRMM ($n = 3$). Bar graphs show mean \pm SEM. Mann-Whitney test (*, $P < 0.05$). **D**, Soluble IFN γ concentration at day 3 was quantified by ELISA. Each symbol represents CD4⁺ T cells from nine patients with multiple myeloma (three SMM, four NDMM, two RRMM). Wilcoxon signed-rank test (*, $P = 0.039$).

Treg-associated genes such as *TGFB1*, *IDO1*, and *NT5E* (*CD73*). We next validated our results with a second cohort of patients by real-time PCR including Treg-related genes (*FOXP3*, *NT5E*, and *IDO1*) as well as well-known immune checkpoints involved in T-cell regulation. Given that TIGIT is a direct FoxP3 target gene, we first confirmed that FoxP3 expression was higher in samples with high TIGIT which was accompanied of an increase in *NT5E* (*CD73*) and *IDO1* mRNA expression (Fig. 5E). We also found increased levels of other immune checkpoints such as *CTLA-4*, *PDCD1*, *HAVCR2* (*TIM-3*), and *LAG3* in samples with higher expression of TIGIT which could be explained by a higher frequency of Tregs and effectors T cells with exhausted phenotype in a subgroup of patients expressing higher levels of TIGIT. Therefore, a subset of patients with multiple myeloma showed higher TIGIT

expression that correlated with higher levels of key mediators involved in immune regulation, which may indicate that response to TIGIT blockade could be more effective in a specific subgroup of patients.

Response to TIGIT blockade in ex vivo BM samples from patients with multiple myeloma is associated to nectin-2 expression on malignant PCs

Given the wide heterogeneity in expression of TIGIT and its ligands found at protein level, we wanted to assess whether response to TIGIT blockade depends on the expression of the components of the TIGIT axis. We incubated 32 freshly isolated BM cells from patients with SMM ($n = 5$), NDMM ($n = 15$), and RRMM ($n = 12$) in the presence of neutralizing anti-TIGIT mAb for 24 hours and we measured the

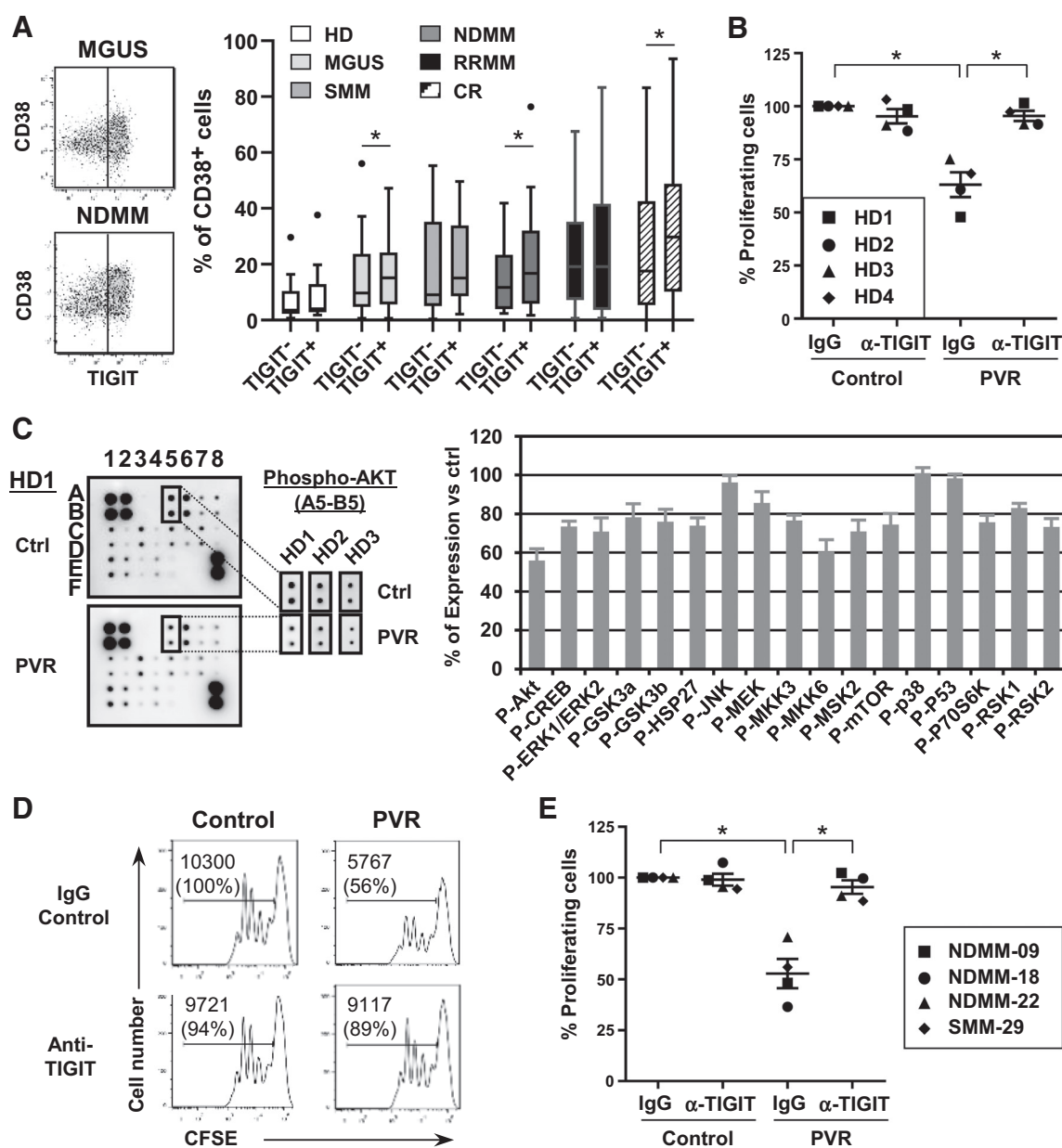


Figure 4.

TIGIT blockade reverses PVR-induced T-cell inhibition in CD8⁺ T cells from patients with multiple myeloma. **A**, Surface expression of activation marker CD38 on BM TIGIT⁻ and TIGIT⁺ CD8⁺ T cells in patients with MGUS ($n = 27$), SMM ($n = 15$), newly diagnosed multiple myeloma ($n = 24$), relapsed/refractory multiple myeloma ($n = 25$), and patients with multiple myeloma in CR ($n = 22$). Wilcoxon matched-pairs signed-rank test (*, $P < 0.05$). **B**, CD8⁺ T cells were isolated from peripheral blood of healthy donors ($n = 4$), stained with CFSE and preincubated with RPMI medium with 10% human serum, in the presence of immobilized PVR (200 ng/mL) and soluble neutralizing anti-TIGIT mAb (10 μ g/mL) or isotype control. After 1 hour, cells were stimulated with CD2/CD3/CD28 MACSIBead particles (bead-to-cell ratio 1:1) and IL2 (10 U/mL). After 4 days, proliferating cells were measured by flow cytometry. Values obtained after TIGIT blockade were normalized to isotype control (as 100%) and percentages of change are depicted ($n = 4$). Kruskal-Wallis test (*, $P < 0.05$). **C**, Changes in phosphorylation of intracellular mediators of T-cell signaling pathways were assessed in CD8⁺ T cells from healthy donors ($n = 3$), incubated onto immobilized PVR (200 ng/mL) for 18 hours and then stimulated with CD2/CD3/CD28 MACSIBead particles for 30 minutes. Cell lysates were incubated on phosphorylation arrays overnight and phosphorylation proteins were detected by duplicate as follows: A1-B1-A2-B2: positive controls; A3-B3-A4-B4: negative controls; A5-B5: AKT1 (p-S473); A6-B6: CREB1 (p-S133); A7-B7: ERK1 (p-T202/Y204)/ERK2 (p-Y185/Y187); A8-B8: GSK3a (p-S21); C1-D1: GSK3b (p-S9); C2-D2: HSP27 (p-S82); C3-D3: JNK (p-T183); C4-D4: MEK (p-S217/221); C5-D5: MKK3 (p-S189); C6-D6: MKK6 (p-S207); C7-D7: MSK2 (p-S360); C8-D8: mTOR (p-S2448); E1-F1: p38 (p-T180/Y182); E2-F2: p53 (p-S15); E3-F3: P70S6K (p-T421/S424); E4-F4: RSK1 (p-S380); E5-F5: RSK2 (p-S386); E6-F6-E7-F7-E8-F8: negative controls. Representative membranes and quantification of three independent experiments are shown. **D**, CFSE proliferation assay with peripheral blood CD8⁺ T cells from a patient with multiple myeloma, representative experiment in the same conditions as in **B**. **E**, Summarized data from proliferation assays with CD8⁺ T cells from four patients with multiple myeloma. A single data point represents the triplicate mean of each patient. Kruskal-Wallis test (*, $P < 0.05$).

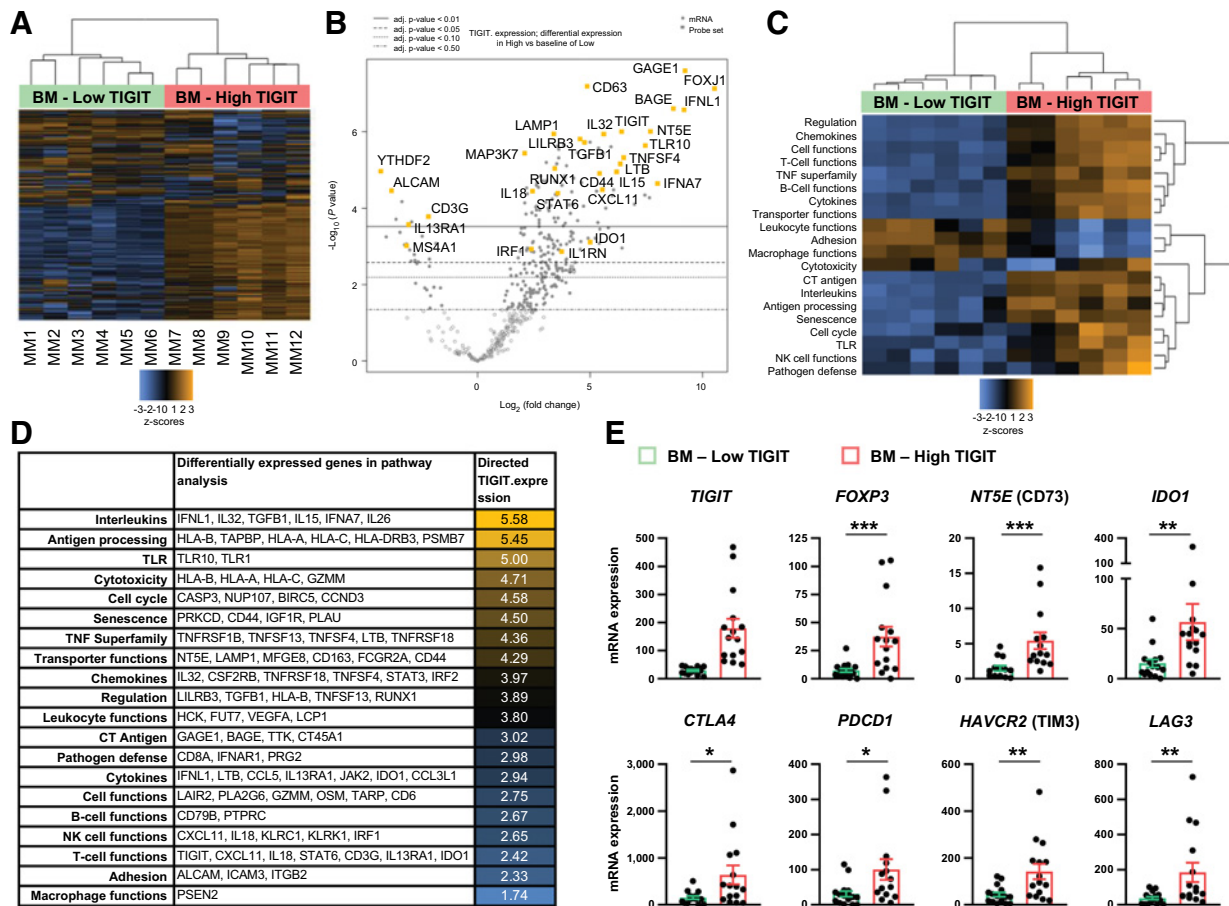


Figure 5.

High levels of TIGIT gene expression are associated to upregulation of genes involved in T-cell function and cytotoxicity in the BM cells from patients with multiple myeloma. **A**, Hierarchical clustering and heatmap of genes differentially expressed between CD138-depleted BM samples with low and high TIGIT expression. Columns correspond to BM samples from individual patients with multiple myeloma ($n = 12$) assessed with the NanoString PanCancer Immune Profiling Panel of 770 genes. **B**, Volcano plot of baseline gene expression displaying the \log_2 fold difference of the median gene expression between BM samples with high and low TIGIT expression. Positive values indicate higher expression in TIGIT-high BM samples; negative values indicate higher expression in the TIGIT-low samples. The y-axis shows $-\log_{10}$ -transformed P values, statistical significance is observed for genes above the solid line ($P < 0.01$) and the dashed line ($P < 0.05$). Every dot represents one gene (complete gene list is shown in Supplementary Table S2). **C**, Pathway analysis showed differences in patient signature based on TIGIT expression. **D**, Ranked list of pathways associated to samples with higher TIGIT expression. **E**, Treg-associated genes validated by real-time PCR in a second cohort of patients with multiple myeloma ($n = 31$). Mann-Whitney test (*, $P < 0.05$; **, $P < 0.01$).

number of malignant PCs by absolute quantification. We found that the decrease in malignant PCs in response to TIGIT blockade ranged from 0% to -32.5% (median -9.5%; **Fig. 6A**). A higher nectin-2 expression correlated with a better response to TIGIT blockade (**Fig. 6B**). Indeed, patients with a decrease in PC number higher than the median (responders) showed a significant increase in nectin-2 but not in PVR (**Fig. 6C**). Accordingly, a higher expression of nectin-2 but not PVR on PCs negatively correlated with the total number of malignant PCs (**Fig. 6D**). Surprisingly, responders also showed lower frequency of BM TIGIT⁺CD4⁺ T cells and lower expression of total TIGIT⁺ cells in the BM (**Fig. 6E**). To assess whether lower frequency of BM TIGIT⁺CD4⁺ T cells in responders was associated to lower frequency of Tregs, when possible we also analyzed the CD3⁺CD4⁺CD127^{low}CD25^{high} T cells in the BM. Indeed, our results showed that responders had a significant lower percentage of CD3⁺CD4⁺CD127^{low}CD25^{high} T cells than nonresponders ($n = 5$ vs $n = 7$, Mann-Whitney test; $P = 0.017$; Supplementary Fig. S2). Thus,

TIGIT blockade was more efficient in a subset of patients with higher expression of nectin-2 on malignant PCs and lower percentage of TIGIT⁺CD4⁺ T cells in BM, which may identify patients with multiple myeloma who may have a better response to TIGIT blockade.

Discussion

Inhibitory checkpoint TIGIT has become an attractive target for cancer immunotherapy (28, 29). We previously reported that ligation to ITIM-bearing receptor TIGIT triggers a negative intrinsic signaling that leads to decrease in proinflammatory cytokines and T-cell growth arrest (23). Because TIGIT blockade promotes tumor regression in a number of mouse tumor models (22, 27, 34), several ongoing clinical trials to treat advanced/metastatic solid tumors are currently evaluating safety and tolerability of anti-TIGIT mAbs (35). In multiple myeloma, recent preclinical studies with multiple myeloma cell lines and mouse models have shown promising results (32, 34) and an

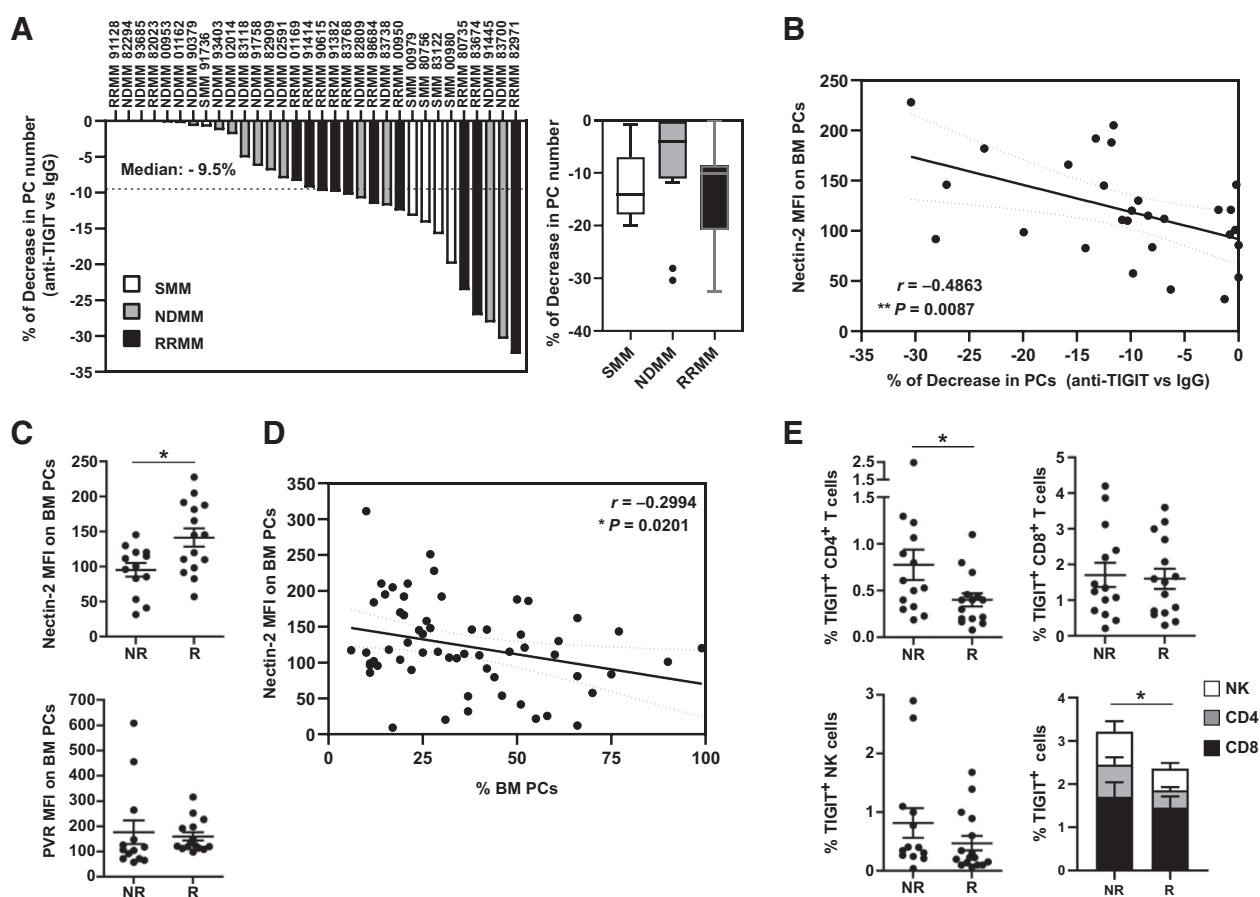


Figure 6.

TIGIT blockade in *ex vivo* BM model from patients with multiple myeloma. **A**, Freshly isolated BM cells from 32 patients with SMM ($n = 5$), NDMM ($n = 15$), and RRMM ($n = 12$) were cultured in the presence of neutralizing anti-TIGIT mAb or isotype control for 24 hours. Number of malignant PCs obtained after TIGIT blockade were normalized to isotype control and percentages of change are depicted. **B**, Pearson correlation between percentage of decrease in PC number and expression of nectin-2 on malignant PCs. **C**, Expression of TIGIT ligands on BM PCs in patients with a decrease in PCs higher than the median (responders, R) versus nonresponders (NR). Unpaired *t* test (*, $P < 0.05$). **D**, Pearson correlation between percentage of PCs and expression of nectin-2 on malignant PC surface in patients with multiple myeloma (SMM $n = 13$, NDMM $n = 23$, RRMM $n = 18$; *, $P < 0.05$). **E**, *Ex vivo* frequencies of TIGIT⁺ CD4⁺ T cells, TIGIT⁺ CD8⁺ T cells, TIGIT⁺ NK cells in BM from responders versus nonresponders to anti-TIGIT mAb. Mann-Whitney test (*, $P < 0.05$). Cumulative frequency of TIGIT⁺ cells in BM. Unpaired *t* test (*, $P < 0.05$).

ongoing phase I/II randomized trial for patients with relapsed refractory multiple myeloma (NCT04150965) will evaluate the immunologic effects and safety of two agents, anti-LAG-3 and anti-TIGIT, as single agents and in combination with pomalidomide and dexamethasone. However, little is known about the expression patterns and functional roles of TIGIT and its ligands in the BM of patients with multiple myeloma. Here, we first characterized TIGIT expression on BM CD4⁺ T cells, CD8⁺ T cells, and NK cells as well as both TIGIT ligands nectin-2 and PVR at sequential stages of myeloma progression. Interestingly, patients with the premalignant condition SMM showed lower TIGIT expression on CD4⁺ T cells and TIGIT expression positively correlated with number of malignant PCs suggesting that TIGIT blockade may activate immune response against malignant PCs in patients with multiple myeloma.

To achieve a successful response to immune checkpoint blockade, patient immune status will play a major role. However, a variety of immune alterations has been reported in patients with multiple myeloma affecting B-cell differentiation, cytotoxic CD8⁺ T-cell response (36), dendritic cell costimulation (37), and dysfunctional regulatory FoxP3⁺ T cells (Tregs; ref. 38). Our study supports a role for

anti-TIGIT therapy in enhancing effector CD4⁺ T-cell proliferation and stimulating IFN γ production in both asymptomatic and symptomatic patients. Unlike CTLA-4 blockade (39), we found that TIGIT targeting caused a significant depletion of FoxP3⁺ Treg cells. Moreover, we demonstrated that PVR ligation triggered a potent negative signaling through TIGIT impairing CD8⁺ T-cell proliferation which could be reversed by TIGIT blockade. Accordingly, recent studies with multiple myeloma mouse models showed that TIGIT blockade prevented myeloma escape after stem cell transplantation (34) and restored CD8⁺ T-cell immunity (32). Furthermore, unlike PD-1, TIGIT was found highly expressed on NK cells in BM suggesting that TIGIT blockade could effectively activate NK-cell cytotoxicity in multiple myeloma (40). Therefore, TIGIT neutralization may act at different levels to reinvigorate peripheral T cells and NK cells to mount the anti-multiple myeloma immune response.

However, in the BM microenvironment, multiple immune suppressive mechanisms are taking place that may jeopardize the efficacy of TIGIT blockade in achieving malignant cell death. Indeed, we found patients who remain unresponsive to TIGIT blockade, which is consistent with the heterogeneity in CD138⁺ BM cells observed by

gene expression profiling. In a recent study, Guillerey and colleagues reported that TIGIT blockade in CD138⁺ BM cells from patients with multiple myeloma stimulated with anti-CD3/CD28/CD2 microbeads and anti-TIGIT mAb significantly increased production of proinflammatory cytokines such as IFN γ , IL2, and TNF α concluding that TIGIT blockade improves CD8⁺ T-cell functions in patients with multiple myeloma (32). In our experiments with CD138⁺ BM cells, we evaluated TIGIT blockade without exogenous activation to mimic the effect of anti-TIGIT mAb administration to patients and we assessed differences in response to treatment based on decrease of BM PC number. Thus, we found that TIGIT neutralization caused malignant PC cell death in patients with higher expression of nectin-2 on malignant PCs and lower frequency of TIGIT⁺ BM cells. Therefore, although a number of preclinical models have provided the rationale for TIGIT blockade in multiple myeloma, it is crucial to evaluate of the antitumor efficacy of neutralizing anti-TIGIT antibodies with primary tumor cells and autologous immune cells that may show defective functions compared with healthy immune cells. Taking into account patient immune status and the heterogeneity found in BM compartment may anticipate mechanisms of resistance to checkpoint blockade (41).

Intriguingly, our study also showed that the roles of both TIGIT ligands nectin-2 and PVR may not be redundant in multiple myeloma. Here, we report distinct expression patterns in the BM and a higher nectin-2 expression on PCs associated to better response to TIGIT blockade. Indeed, the TIGIT interaction with PVR has higher affinity compared with TIGIT/nectin-2 interaction (20, 21, 42, 43). Interestingly, a recent study proposed that nectin-2–PVRIG and PVR–TIGIT as two nonredundant inhibitory signaling nodes (44). Further characterization of nectin-2–TIGIT interaction at functional level would be needed to better understand both T cell–cancer cell contact and T cell–antigen-presenting cells interaction.

The remarkable responses to immune checkpoint blockade are currently limited to a minority of patients and indications (41). In patients with multiple myeloma, BM cells showed a heterogeneous immune signature indicating that efficacy of neutralizing anti-TIGIT mAb may differ between patients. An ongoing clinical trial evaluating TIGIT neutralization (NCT04150965) may shed more light on predictive biomarkers such as nectin-2 and PVR on PCs. Hence, further

research in this field would be essential to better understand the mechanisms controlled by the TIGIT axis which will lead to identify eligible patients for this targeted strategy and improve their clinical outcomes in this new era of cancer immunotherapies.

Disclosure of Potential Conflicts of Interest

M.T. Cibeira reports personal fees from Janssen (Educational lecture and advisory board), Celgene (Educational lecture), Amgen (Educational lecture), and Akcea (Advisory board) outside the submitted work. A. Prat reports personal fees and nonfinancial support from Nanostring Technologies during the conduct of the study, as well as grants from Roche, and personal fees from Roche, Oncolytics Biotech, Daiichi Sankyo, AstraZeneca, Pfizer, BMS, MSD, and Novartis outside the submitted work. L. Rosinol reports personal fees from Janssen, Celgene, Amgen, and Takeda outside the submitted work. C. Fernández de Larrea reports grants and personal fees from Janssen, Takeda, Amgen, and BMS outside the submitted work. No potential conflicts of interest were disclosed by the other authors.

Authors' Contributions

E. Lozano: Conceptualization, supervision, funding acquisition, validation, investigation, methodology, writing-original draft, writing-review and editing. **M.-P. Mena:** Conceptualization, software, validation, investigation, methodology, writing-original draft. **T. Diaz:** Resources, investigation, methodology. **B. Martin-Antonio:** Validation, investigation. **S. León:** Methodology. **L.-G. Rodríguez-Lobato:** Resources, data curation, formal analysis. **A. Oliver-Caldés:** Resources, data curation, investigation. **M.T. Cibeira:** Resources, data curation, investigation. **J. Bladé:** Supervision, writing-original draft. **A. Prat:** Resources, software, formal analysis, investigation. **L. Rosinol:** Conceptualization, supervision, investigation, writing-original draft, project administration. **C. Fernández de Larrea:** Conceptualization, supervision, funding acquisition, investigation, writing-original draft, project administration, writing-review and editing.

Acknowledgments

This work was supported in part by Grants PI16/00423 and PI19/00669 from Instituto de Salud Carlos III (Ministerio de Economía y Competitividad, co-funded by Fondo Europeo de Desarrollo Regional (FEDER)-Una manera de Hacer Europa) and the CERCA Programme/Generalitat de Catalunya.

The costs of publication of this article were defrayed in part by the payment of page charges. This article must therefore be hereby marked *advertisement* in accordance with 18 U.S.C. Section 1734 solely to indicate this fact.

Received November 13, 2019; revised April 8, 2020; accepted June 3, 2020; published first June 8, 2020.

References

- Blade J, Cibeira MT, Fernandez de Larrea C, Rosinol L. Multiple myeloma. *Ann Oncol* 2010;21:vii313–9.
- International Myeloma Working Group. Criteria for the classification of monoclonal gammopathies, multiple myeloma and related disorders: a report of the International Myeloma Working Group. *Br J Haematol* 2003;121:749–57.
- Blade J, Dimopoulos M, Rosinol L, Rajkumar SV, Kyle RA. Smoldering (asymptomatic) multiple myeloma: current diagnostic criteria, new predictors of outcome, and follow-up recommendations. *J Clin Oncol* 2010;28:690–7.
- Kyle RA, Remstein ED, Therneau TM, Dispenzieri A, Kurtin PJ, Hodnefield JM, et al. Clinical course and prognosis of smoldering (asymptomatic) multiple myeloma. *N Engl J Med* 2007;356:2582–90.
- Caers J, Fernandez de Larrea C, Leleu X, Heusschen R, Zojer N, Decaux O, et al. The changing landscape of smoldering multiple myeloma: a European perspective. *Oncologist* 2016;21:333–42.
- Blade J, Fernandez de Larrea C, Rosinol L. Incorporating monoclonal antibodies into the therapy of multiple myeloma. *J Clin Oncol* 2012;30:1904–6.
- Kumar SK, Dispenzieri A, Lacy MQ, Gertz MA, Buadi FK, Pandey S, et al. Continued improvement in survival in multiple myeloma: changes in early mortality and outcomes in older patients. *Leukemia* 2014;28:1122–8.
- Costa LJ, Brill IK, Omel J, Godby K, Kumar SK, Brown EE. Recent trends in multiple myeloma incidence and survival by age, race, and ethnicity in the United States. *Blood Adv* 2017;1:282–7.
- Blade J, Rosinol L, Fernandez de Larrea C. How I treat relapsed myeloma. *Blood* 2015;125:1532–40.
- Sharpe AH, Abbas AK. T-cell costimulation—biology, therapeutic potential, and challenges. *N Engl J Med* 2006;355:973–5.
- Lozano E, Diaz T, Mena MP, Sune G, Calvo X, Calderon M, et al. Loss of the immune checkpoint CD85/LILRB1 on malignant plasma cells contributes to immune escape in multiple myeloma. *J Immunol* 2018;200:2581–91.
- Hodi FS, O'Day SJ, McDermott DF, Weber RW, Sosman JA, Haanen JB, et al. Improved survival with ipilimumab in patients with metastatic melanoma. *N Engl J Med* 2010;363:711–23.
- Antonia SJ, Larkin J, Ascierto PA. Immuno-oncology combinations: a review of clinical experience and future prospects. *Clin Cancer Res* 2014;20:6258–68.
- Pianko MJ, Moskowitz AJ, Lesokhin AM. Immunotherapy of lymphoma and myeloma: facts and hopes. *Clin Cancer Res* 2018;24:1002–10.
- Chung DJ, Pronschinske KB, Shyer JA, Sharma S, Leung S, Curran SA, et al. T-cell exhaustion in multiple myeloma relapse after autotransplant: optimal timing of immunotherapy. *Cancer Immunol Res* 2016;4:61–71.

16. Suen H, Brown R, Yang S, Weatherburn C, Ho PJ, Woodland N, et al. Multiple myeloma causes clonal T-cell immunosenescence: identification of potential novel targets for promoting tumour immunity and implications for checkpoint blockade. *Leukemia* 2016;30:1716–24.
17. Suen H, Brown R, Yang S, Ho PJ, Gibson J, Joshua D. The failure of immune checkpoint blockade in multiple myeloma with PD-1 inhibitors in a phase 1 study. *Leukemia* 2015;29:1621–2.
18. Usmani SZ, Schjesvold F, Oriol A, Karlin L, Cavo M, Rifkin RM, et al. Pembrolizumab plus lenalidomide and dexamethasone for patients with treatment-naïve multiple myeloma (KEYNOTE-185): a randomised, open-label, phase 3 trial. *Lancet Haematol* 2019;6:e448–58.
19. Mateos MV, Blacklock H, Schjesvold F, Oriol A, Simpson D, George A, et al. Pembrolizumab plus pomalidomide and dexamethasone for patients with relapsed or refractory multiple myeloma (KEYNOTE-183): a randomised, open-label, phase 3 trial. *Lancet Haematol* 2019;6:e459–69.
20. Stanietsky N, Simic H, Arapovic J, Toporik A, Levy O, Novik A, et al. The interaction of TIGIT with PVR and PVRL2 inhibits human NK cell cytotoxicity. *Proc Natl Acad Sci U S A* 2009;106:17858–63.
21. Yu X, Harden K, Gonzalez LC, Francesco M, Chiang E, Irving B, et al. The surface protein TIGIT suppresses T cell activation by promoting the generation of mature immunoregulatory dendritic cells. *Nat Immunol* 2009;10:48–57.
22. Joller N, Hafler JP, Brynedal B, Kassam N, Spoerl S, Levin SD, et al. Cutting edge: TIGIT has T cell-intrinsic inhibitory functions. *J Immunol* 2011;186:1338–42.
23. Lozano E, Dominguez-Villar M, Kuchroo V, Hafler DA. The TIGIT/CD226 axis regulates human T cell function. *J Immunol* 2012;188:3869–75.
24. Levin SD, Taft DW, Brandt CS, Bucher C, Howard ED, Chadwick EM, et al. Vstm3 is a member of the CD28 family and an important modulator of T-cell function. *Eur J Immunol* 2011;41:902–15.
25. Bottino C, Castriconi R, Pende D, Rivera P, Nanni M, Carnemolla B, et al. Identification of PVR (CD155) and Nectin-2 (CD112) as cell surface ligands for the human DNAM-1 (CD226) activating molecule. *J Exp Med* 2003;198:557–67.
26. Lozano E, Joller N, Cao Y, Kuchroo VK, Hafler DA. The CD226/CD155 interaction regulates the proinflammatory (Th1/Th17)/anti-inflammatory (Th2) balance in humans. *J Immunol* 2013;191:3673–80.
27. Joller N, Lozano E, Burkett PR, Patel B, Xiao S, Zhu C, et al. Treg cells expressing the coinhibitory molecule TIGIT selectively inhibit proinflammatory Th1 and Th17 cell responses. *Immunity* 2014;40:569–81.
28. Blake SJ, Dougall WC, Miles JJ, Teng MW, Smyth MJ. Molecular pathways: targeting CD96 and TIGIT for cancer immunotherapy. *Clin Cancer Res* 2016;22:5183–8.
29. Dougall WC, Kurtulus S, Smyth MJ, Anderson AC. TIGIT and CD96: new checkpoint receptor targets for cancer immunotherapy. *Immunol Rev* 2017;276:112–20.
30. Dixon KO, Schorer M, Nevin J, Etmann Y, Amoozgar Z, Kondo T, et al. Functional anti-TIGIT antibodies regulate development of autoimmunity and antitumor immunity. *J Immunol* 2018;200:3000–7.
31. Kurtulus S, Sakuishi K, Ngiew SF, Joller N, Tan DJ, Teng MW, et al. TIGIT predominantly regulates the immune response via regulatory T cells. *J Clin Invest* 2015;125:4053–62.
32. Guillerey C, Harjunpaa H, Carrie N, Kassem S, Teo T, Miles K, et al. TIGIT immune checkpoint blockade restores CD8(+) T-cell immunity against multiple myeloma. *Blood* 2018;132:1689–94.
33. Kumar S, Paiva B, Anderson KC, Durie B, Landgren O, Moreau P, et al. International Myeloma Working Group consensus criteria for response and minimal residual disease assessment in multiple myeloma. *Lancet Oncol* 2016;17:e328–46.
34. Minnie SA, Kuns RD, Gartlan KH, Zhang P, Wilkinson AN, Samson L, et al. Myeloma escape after stem cell transplantation is a consequence of T-cell exhaustion and is prevented by TIGIT blockade. *Blood* 2018;132:1675–88.
35. Kucan Brlic P, Lenac Rovis T, Cinamon G, Tsukerman P, Mandelboim O, Jonjic S. Targeting PVR (CD155) and its receptors in anti-tumor therapy. *Cell Mol Immunol* 2019;16:40–52.
36. Maecker B, Anderson KS, von Bergwelt-Baildon MS, Weller E, Vonderheide RH, Richardson PG, et al. Viral antigen-specific CD8+ T-cell responses are impaired in multiple myeloma. *Br J Haematol* 2003;121:842–8.
37. Brown RD, Pope B, Murray A, Esdale W, Sze DM, Gibson J, et al. Dendritic cells from patients with myeloma are numerically normal but functionally defective as they fail to up-regulate CD80 (B7-1) expression after huCD40LT stimulation because of inhibition by transforming growth factor-beta1 and interleukin-10. *Blood* 2001;98:2992–8.
38. Prabhala RH, Neri P, Bae JE, Tassone P, Shammas MA, Allam CK, et al. Dysfunctional T regulatory cells in multiple myeloma. *Blood* 2006;107:301–4.
39. Kavanagh B, O'Brien S, Lee D, Hou Y, Weinberg V, Rini B, et al. CTLA4 blockade expands FoxP3+ regulatory and activated effector CD4+ T cells in a dose-dependent fashion. *Blood* 2008;112:1175–83.
40. Paiva B, Azpilikueta A, Puig N, Ocio EM, Sharma R, Oyajobi BO, et al. PD-L1/PD-1 presence in the tumor microenvironment and activity of PD-1 blockade in multiple myeloma. *Leukemia* 2015;29:2110–3.
41. Pitt JM, Vetizou M, Daillere R, Roberti MP, Yamazaki T, Routy B, et al. Resistance mechanisms to immune-checkpoint blockade in cancer: tumor-intrinsic and -extrinsic factors. *Immunity* 2016;44:1255–69.
42. Stengel KF, Harden-Bowles K, Yu X, Rouge L, Yin J, Comps-Agrar L, et al. Structure of TIGIT immunoreceptor bound to poliovirus receptor reveals a cell-cell adhesion and signaling mechanism that requires cis-trans receptor clustering. *Proc Natl Acad Sci U S A* 2012;109:5399–404.
43. Deuss FA, Gully BS, Rossjohn J, Berry R. Recognition of nectin-2 by the natural killer cell receptor T cell immunoglobulin and ITIM domain (TIGIT). *J Biol Chem* 2017;292:11413–22.
44. Whelan S, Ophir E, Kotturi MF, Levy O, Ganguly S, Leung L, et al. PVRIG and PVRL2 are induced in cancer and inhibit CD8(+) T-cell function. *Cancer Immunol Res* 2019;7:257–68.